CHEMISTRY
A EUROPEAN JOURNAL

DOI: 10.1002/chem.200700369

α-Phenyl-*N*-*tert*-butylnitrone-Type Derivatives Bound to β-Cyclodextrins: Syntheses, Thermokinetics of Self-Inclusion and Application to Superoxide Spin-Trapping

David Bardelang,*[a] Laurence Charles,[b] Jean-Pierre Finet,[a] Laszlo Jicsinszky,[c] Hakim Karoui,[a] Sylvain R. A. Marque,*[a] Valérie Monnier,[b] Antal Rockenbauer,[d] Roseline Rosas,[b] and Paul Tordo[a]

In memory of Dr. Jean-Pierre Finet, who passed away on April 15th, 2007

Abstract: α-Phenyl-*N*-*tert*-butylnitrone (PBN) derivatives bound to β-cyclodextrin derivatives have been synthesized. Inclusion of the PBN group into the β-cyclodextrin moiety is host- and temperature-dependent. In the case of the nitrone linked to permethylated cyclodextrin (Me3CD-PBN), the thermokinetic parameters are in favour of a slow chemical exchange between a tight and a loose complex. In contrast, 2,6-di-*O*-Me-β-cyclodextrin-grafted PBN (Me2CD-PBN) exists either in a fast exchange or as a strongly self-associated complex. The covalent cyclodextrin–PBN compounds have been used to trap carbon and oxygen-centred free radicals. The self-associated forms of the β-CD-spin-traps are compatible with effective spin-trapping, affording spin-adducts with enhanced EPR signal intensities relative to noncovalent CD–nitrone systems or the nitrone alone. This kind of cyclodextrin-bound nitrone is the first type of covalent supramolecular spin-trap and should open new possibilities for the study of biological free radicals in vivo.

Keywords: cyclodextrins · EPR spectroscopy · spin trapping · superoxide · supramolecular chemistry

Introduction

Detection of oxygen-centred free radicals is of particular interest for better understanding of their importance in the physiological control of cell functions[1] and in many pathologies such as neurodegenerative disorders,[2] hypertension,[3] cancer[4] or diabetes.[5] Over the years, it has emerged that many of these diseases are related to the occurrence of oxidative stress situations,[6] due to an imbalanced production of superoxide radical anion ($O_2^{\bullet -}$).[7] One challenge of the last decade was to develop new techniques and subsequently new spin-traps for study of $O_2^{\bullet -}$ in vivo. On the other hand, it has been reported that cyclodextrins (CDs) represent powerful supramolecular assistants[8] of superoxide trapping in terms of spin-adduct stabilization, EPR signal intensity enhancement and partial protection of the spin-adducts against L-ascorbate reduction.[9–12] However, the concentration of methylated β-cyclodextrins required for observation of such effects (50 mM) is physiologically unsuitable for in vivo applications. Another drawback is the presence in biological fluids of many potential guest molecules that can compete intensively for guest accommodation with the desired spin-labelled adducts.

[a] Dr. D. Bardelang, Dr. J.-P. Finet, Dr. H. Karoui, Dr. S. R. A. Marque, Prof. P. Tordo
UMR 6517 CNRS et Aix-Marseille Université
Faculté de Saint-Jérôme
Case 521, Avenue Escadrille Normandie Niemen
13397 Marseille Cedex 20 (France)
Fax: (+33) 491-288-758
E-mail: david.bardelang@nrc-cnrc.gc.ca
sylvain.marque@univ-provence.fr

[b] Prof. L. Charles, Dr. V. Monnier, R. Rosas
Spectropole, Faculté de Saint-Jérôme
Case 511, Marseille Cedex 20 (France)

[c] Dr. L. Jicsinszky
Cyclolab Ltd., PO Box 435, 1525 Budapest (Hungary)

[d] Prof. A. Rockenbauer
Chemical Research Center, Institute of Structural Chemistry
PO Box 17, 1525 Budapest (Hungary)

Supporting information for this article is available on the WWW under http://www.chemeurj.org/ or from the author: Syntheses of **7** and **10**, and their precursors, mass spectrometry data, NMR and EPR procedures.

To address these limitations, a covalent model with the nitrone spin-trap attached to a monofunctionalized CD is proposed in this paper. Thus, Me2CD-PBN (**7**) and Me3CD-PBN (**10**), derivatives of α-phenyl-*N*-*tert*-butylnitrone (PBN) bound to 2,6-di-*O*-Me-β-cyclodextrin (DIMEB-derived)[13] and permethylated β-cyclodextrin (TRIMEB-derived), respectively, have been synthesized. Hence, smaller amounts of CD should be required for complexation of the spin-adduct, which should furthermore be better stabilized because of the greater affinity of the CD cavity towards accommodation of the spin-adduct rather than the nitrone.[11,12]

Results and Discussion

Synthesis: α-Phenyl-*N*-*tert*-butylnitrone (PBN), a linear nitrone, was selected i) for its simplicity for evaluation of the feasibility of preparation of a covalent nitrone–CD system, ii) because of its complementary structure toward the cavity of β-CD derivatives,[11,14] and iii) to determine the influence of the grafted hosts on the superoxide spin-trapping properties in relation to those of noncovalent PBN–CD systems. By considering DIMEB and TRIMEB derivatives as macrocyclic hosts, we also expected to favour spin-adduct complexation over spin-trap complexation. Selective chemical modification of nitrones without affecting the nitrone moiety is usually difficult to achieve, due to the pronounced reactivity of the nitrone function.[15] The easy reaction of a hydroxy group, present on the *tert*-butyl part of the 1-phenyl-2-methylpropyl-1,1-dimethylethyl-2-nitroxide free radical, with disuccinimidyl carbonate (DSC) encouraged us to attempt the direct activation of a hydroxy-PBN derivative by treatment with DSC.[16] Thus, treatment of **1**[14] with DSC in acetonitrile in the presence of triethylamine (TEA) afforded the side-chain activated nitrone **3** (Scheme 1). Selective methylation in the 2- and the 6-positions of cyclodextrin derivative **4**[17] by a modified Szejtli protocol using dimethyl sulfate in the presence of barium oxide and barium hydroxide, in equivalent volumes of DMF and DMSO, afforded compound **5**. This compound was reduced to the amine derivative **6** by catalytic transfer hydrogenation with hydrazine monohydrate in the presence of Pd/C in methanol.[18] The reaction between amine **6** and the carbonate derivative **3** in the presence of TEA in anhydrous dichloromethane afforded Me2CD-PBN (**7**). Overmethylation products were almost completely removed by flash chromatography on silica gel. Mass spectrometry analyses of commercial samples of DIMEB also revealed the presence of overmethylation products, which do not alter the recognition properties of the CD. In fact, only one or two supplementary methylations in the 3-position are not sufficient to disrupt the hydrogen bond network responsible for the pseudo-rigid preorganized β-CD- and DIMEB-type conformations, unlike in the case of the TRIMEB type.

Preparation of the analogous Me3CD-PBN (**10**) was achieved by applying the same sequence of reduction and condensation (Scheme 1) to 6-monodeoxy-6-monoazido-Me_3CD (**8**).

The proposed structures of **7** and **10** were supported by the analytical data such as, for example, the mass spectrum of Me3CD-PBN (**10**), displayed in Figure 1 (for MS/MS details, see Supporting Information).

Abstract in French: *α-Phenyl-*N-tert-*butylnitrones (PBNs) attaché à Des β-cyclodextrines fonctionaliséees par l'(α)-phenyl-*N-*tert-butylnitrone (PBN) ont été préparées pour la première fois. Les processus d'inclusion du fragment PBN dans la cavité des cyclodextrines dépend du type de cyclodextrines et de la température. Dans le cas d'un fragment PBN attaché a une cyclodextrine perméthylée (Me_3CD-PBN), les paramètres thermodynamiques supportent l'échange lent entre un complexe ayant un fragment PBN fortement associé et un complexe ayant un fragment PBN faiblement associé. Par contre, avec la 2,6-di-*O-Me-β-cyclodextrine portant un groupe PBN (Me2CD-PBN), il est difficile de différencier entre un échange rapide entre un fragment PBN inclus dans la cavité et l'autre a l'extérieur et un complexe avec un fragment PBN fortement associé dans la cavité. Ces systèmes covalents cyclodextrine–PBN se sont révélés être des pièges efficaces à radicaux libres centrés sur le carbone ou sur l'oxygène. Les signaux de RPE des adduits sont nettement plus intenses avec des systèmes covalents qu'avec des systèmes binaires (nitrones+cyclodextrine) ou qu'avec la nitrone pure. Ces molécules sont la première génération de systèmes de ce type et offrent de nouvelles possibilités pour l'étude des radicaux libres in vivo.*

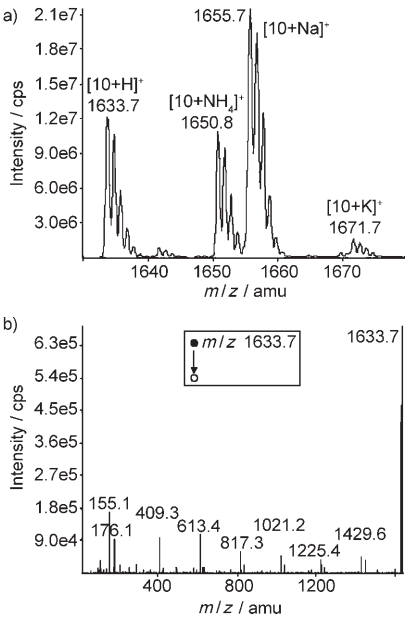

Figure 1. a) Positive electrospray mass spectrum of **10** and b) MS/MS spectrum of $[\mathbf{10}+H]^+$ at *m*/*z* 1633.7

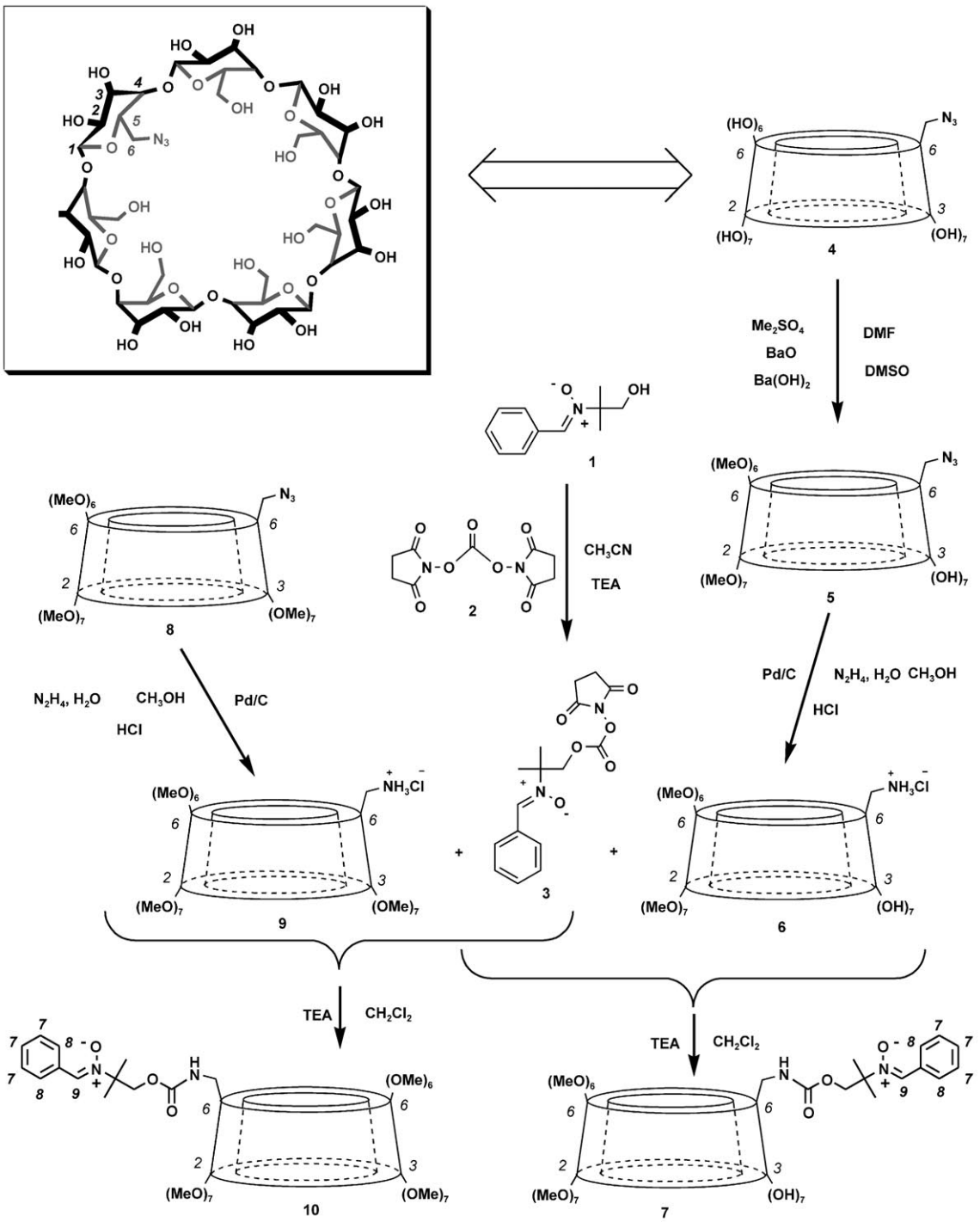

Scheme 1. Synthesis of the CD-PBN derivatives Me2CD-PBN (**7**) and Me3CD-PBN (**10**).

NMR study of PBN/TRIMEB: Before the NMR study of covalent compounds **7** and **10** was addressed, comparison of the influence of the CD substitution on the recognition properties in the two corresponding noncovalent systems was necessary. Interactions in noncovalent bimolecular systems involving PBN and substituted CDs have only been reported for RAMEB (randomly methylated β-cyclodextrin) and DIMEB as hosts.[11] In this latter case, a 1:1 complex was observed and a binding constant of around $80\,M^{-1}$ was found by NMR titration. ^1H NMR titration of the PBN/TRIMEB system was performed with the assumption of a 1:1 complex formation. The chemical shift of the most sensitive (H_9) proton was monitored with increasing CD concentrations. A fast exchange regime was observed and a nonlinear curve fit according to the Macomber model[19–21] gave a very small binding constant of $4\,M^{-1}$ (Figure S9). In

TRIMEB, permethylation of the β-cyclodextrin hydroxy groups results in the loss of rigidity and absence of preorganization of the CD cavity, so the conformations of TRIMEB are less favourable than those of DIMEB for efficient binding of PBN. Indeed, the absence of any hydrogen bonding network in TRIMEB is correlated with the very small value of K_{H9} ($K_{H9}=4\,M^{-1}$) in relation to the previously reported values for DIMEB ($K_1=80\,M^{-1}$)[11] and natural β-CD ($K_1=117\,M^{-1}$).[14]

NMR study of Me2CD-PBN (7): In the ^{1}H NMR spectrum of **7** in D_2O (Figure 2b), the signals of the aromatic protons H_7 and H_8 and the nitronyl proton H_9 are broader than the corresponding signals observed for free PBN in D_2O (Figure 2a). The ^{1}H NMR chemical shift of H_9 in compound **7** is significantly shielded, by up to 0.5 ppm, in comparison with the maximum complexation-induced shift (CIS) reported in the noncovalent PBN/DIMEB case ($\Delta\delta\approx0.41$ ppm).[11] Such a strong upfield shift of H_9[22] is indicative of a deep inclusion of the PBN part inside the CD cavity. The absence of significant changes in the spectrum of **7** (Figure 2b) in the 1–9 mM range of concentrations excluded the formation of intermolecular complexes. At higher concentrations (Figure 2c), however, new signals appeared in the region of H_8 ($\delta=8.28$ ppm) and at $\delta=7.85$ ppm. The lack of signal (see below; Figure 3) in the H_9 region ($\delta=8.05$ ppm) excluded the formation of head-to-tail complexes featuring a non-self-included nitrone fragment. A tentative description of the new species would be a head-to-tail dimer with one nitrone partly included in intermolecular fashion and a second nitrone partly excluded in intramolecular inclusion (Figure 2c). The absence of an H_9 signal around 8 ppm—which would otherwise correspond to the non-included nitrone fragment—at low concentrations led us to consider either the occurrence of a fast exchange between in- and out-complexes or the existence of a strongly bound complex. To obtain deeper insight into these alternatives, we performed two sets of competition experiments with external competitors. In the first series of experiments, DIMEB was used to observe the competition for PBN accommodation between the cavity of Me2CD and the cavity of DIMEB. Addition of DIMEB as an external host led to the appearance of a new signal in the H_8 region (◇, Figure 2d), probably due to intermolecular nitrone–DIMEB complexes (this is further supported by the absence of H_8 and H_9 signals corresponding to free PBN). ^{1}H NMR integration of H_8 indicated that the presence of 10% of intermolecular DIMEB:**7** complex promoted strong self-inclusion of the PBN moiety in the Me2CD cavity, as the included guest can hardly be complexed intermolecularly in spite of the presence of a sixfold excess of competitor. It is worth mentioning that a clear difference is observed for the shift of H_8, although the cavity (DIMEB) used for the intermolecular complex formation is very similar to that in the self-included Me2CD complex. This denotes the high sensitivity of H8 to its chemical environment.

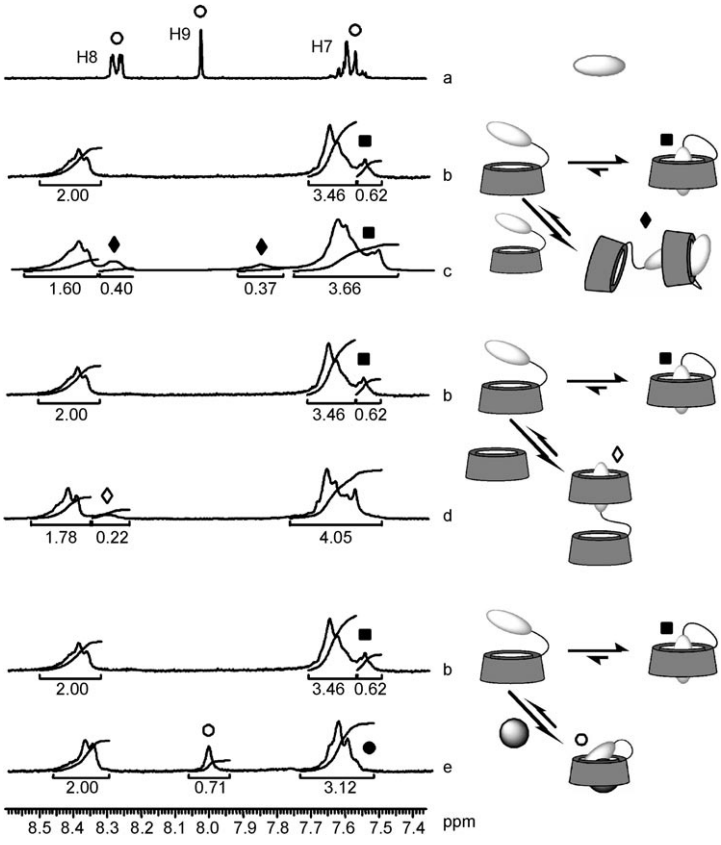

Figure 2. Aromatic parts of ^{1}H NMR spectra in D_2O of a) PBN, b) **7** (2 mM), c) **7** (50 mM), d) **7** (8 mM) with DIMEB (50 mM), and e) **7** (2 mM) with adamantan-1-ol (4.8 mM). Truncated cones are used to symbolize CD derivatives, egg shapes for PBN and spheres for adamantan-1-ol; ◆ and ◇ symbols represent possible species accounting for additional signals; see text.

In the second set of competition experiments, adamantan-1-ol ($K\approx10^4$–$10^5\,M^{-1}$)[23] was used to expel the nitrone moiety outside of the Me2CD cavity. The ^{1}H NMR spectrum of **7** was strikingly modified upon addition of adamantan-1-ol (Figure 2e), with the appearance of a peak at $\delta=7.99$ ppm, corresponding to the non-included nitronyl proton H_9 ($\delta=8.01$ ppm for PBN, and $\delta=7.95$ ppm for H_9 of **10**; see below). However, the only, scarce, modifications observed in the H_8 proton region were not compatible with the induction of complete expulsion of the nitrone moiety by the inclusion of adamantan-1-ol. Indeed, in such a case, an unambiguous signal for H_8 should be observed around 8.25 ppm. Hence, the absence of a δH_8 shift led us to consider the possibility that the cavity may accommodate both the nitrone moiety and the adamantan-1-ol competitor, by pushing only a part of the nitrone moiety outside of the cavity: that is, the nitronyl proton H_9 (Figure 2e). Consequently, this experiment further confirms strong binding of the nitrone moiety in the appended Me2CD cavity. Moreover, an absence of changes in the ^{1}H NMR spectrum was observed when the temperature was increased from 13 to 57 °C (9 mM in water; see below).

NMR study of Me3CD-PBN (10): In contrast with that of molecule **7**, the ^{1}H NMR spectrum of Me3CD-PBN (**10**;

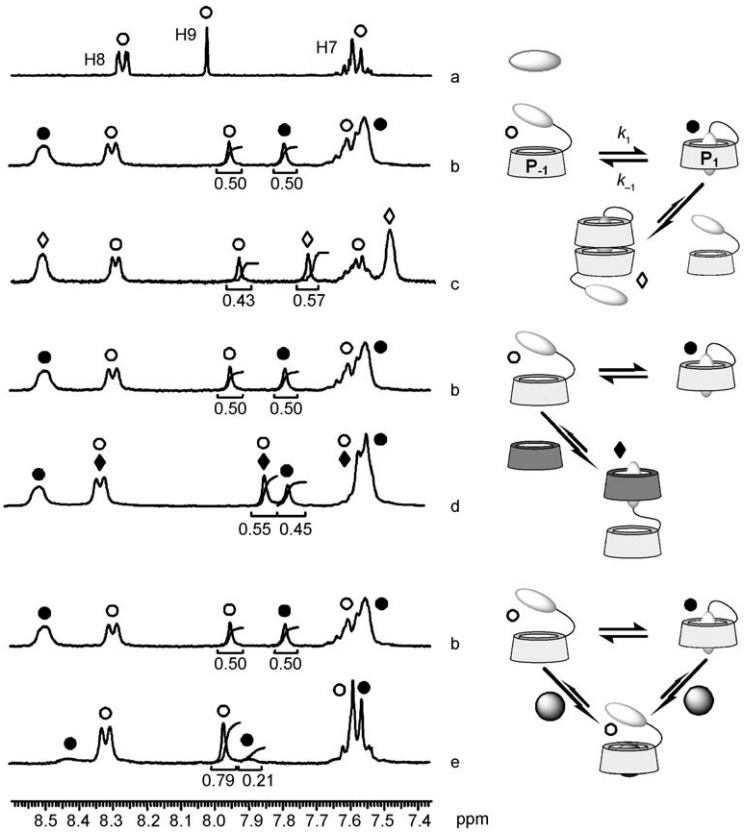

Figure 3. Aromatic part of the ^{1}H NMR spectra in D_2O of a) PBN, b) **10** (2 mM), c) **10** (50 mM), d) **10** (10 mM) with DIMEB (50 mM), and e) **10** (2 mM) with adamantan-1-ol (4.8 mM). Truncated cones are used to symbolize CD derivatives, egg shapes for PBN and spheres for adamantan-1-ol; ◆ and ◇ symbols represent possible species accounting for additional signals; see text.

Figure 3) exhibits several peaks in the region of protons H_8 and H_9 ascribed both to the non-included (or weakly associated; see below) nitrone moiety (broad doublet at $\delta =$ 8.25–8.33 ppm for H_8, singlet at $\delta = 7.95$ ppm for H_9, and multiplet at $\delta = 7.50$–7.64 ppm for H_7 in Figure 3b (○) and to the self-included nitrone moiety (broad singlet at $\delta = 8.51$ ppm for H_8, singlet at $\delta = 7.77$ ppm for H_9, and multiplet at $\delta =$ 7.50–7.64 ppm for H_7 in Figure 3b (●). The occurrence of such kinetically stable host–guest systems has seldom been reported, especially in cases involving host–guest appended compounds.[24]

The HMQC spectrum exhibited additional signals in the aromatic region in comparison with that of the free PBN molecule (Figure S10). The ROESY spectrum showed correlation peaks A and B (Figure 4) between the aromatic protons and methyl groups of the PBN moiety and the inside cavity protons of the CD. These correlation peaks are indicative of a deep inclusion of a nitrone moiety self-included inside the CD cavity.

The absence of significant changes in the ^{1}H NMR spectrum (Figure 3b) upon variation of the concentration of **10** from 0.1 to 10 mM excluded the formation of intermolecular complexes. However, at higher concentrations (50 mM, Figure 3c), new broad singlets (◇) appeared at $\delta = 7.48$ ppm and $\delta = 7.73$ ppm, corresponding to H_7 and H_9, respectively. At the same time, the self-included species disappeared and the amount of non-included (or weakly associated; see below) species decreased slightly. The absence of significant changes for H_8 (no shielding such as observed in the case of **7**), the slight shielding

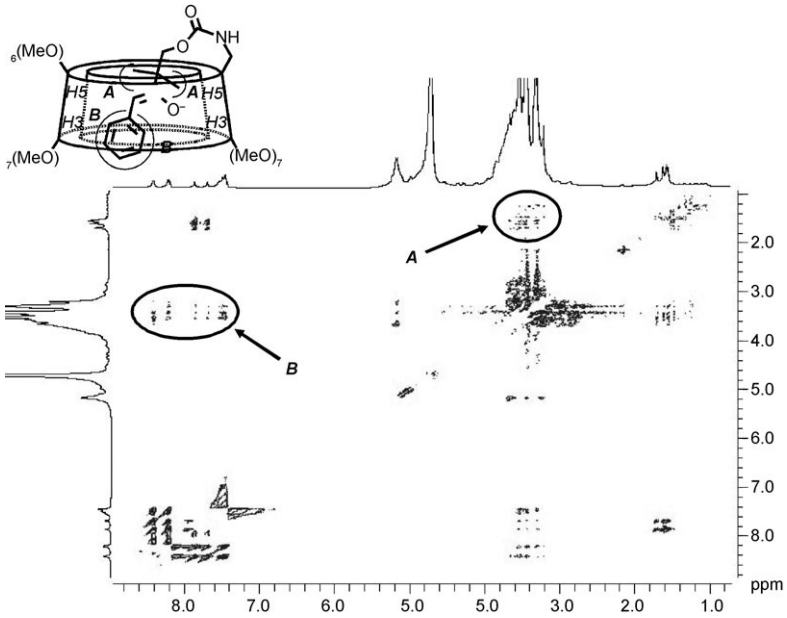

Figure 4. 500 MHz ROESY spectrum of **10** in D_2O (9 mM) illustrating intramolecular ROE cross-correlations due to interactions between the methyl (A) and aromatic (B) protons of the PBN moiety and the protons located inside the Me3CD cavity.

of H_9 and the presence of a new shielded singlet peak for H_7 make the presence of a head-to-tail complex unlikely. On the contrary, a head-to-head complex should increase the shielding of H_7 with minor changes in the region of H_8. Furthermore, such a complex may force the inclusion of the PBN fragment deeper into the cavity, entailing a slightly more shielded H_9 signal. To obtain deeper insight into these inclusion-exclusion processes, we performed competitive experiments using either DIMEB ($K = 80\,\text{M}^{-1}$) to pull the nitrone fragment out of the Me3CD cavity to form an intermolecular complex inside the DIMEB, or adamantan-1-ol ($K \approx 10^4$–$10^5\,\text{M}^{-1}$[23]) to push the nitrone fragment out of the Me3CD cavity. In the presence of an excess of DIMEB, the signals of H_8 and H_9 previously attributed to the non-included (or weakly associated; see below) nitrone conformer (○ in Figure 3b) were shifted significantly (◆ in Figure 3d). However, the signal of the self-included nitrone fragment was only slightly affected (that is, a slight decrease in the amount of the self-included species). The shielding only of the H_9 proton in the presence of DIMEB is in agreement with a fast exchange between the non-included (or weakly associated; see below) nitrone fragment and DIMEB. This indicates that the self-included complex is strong enough to compete with the DIMEB complex.

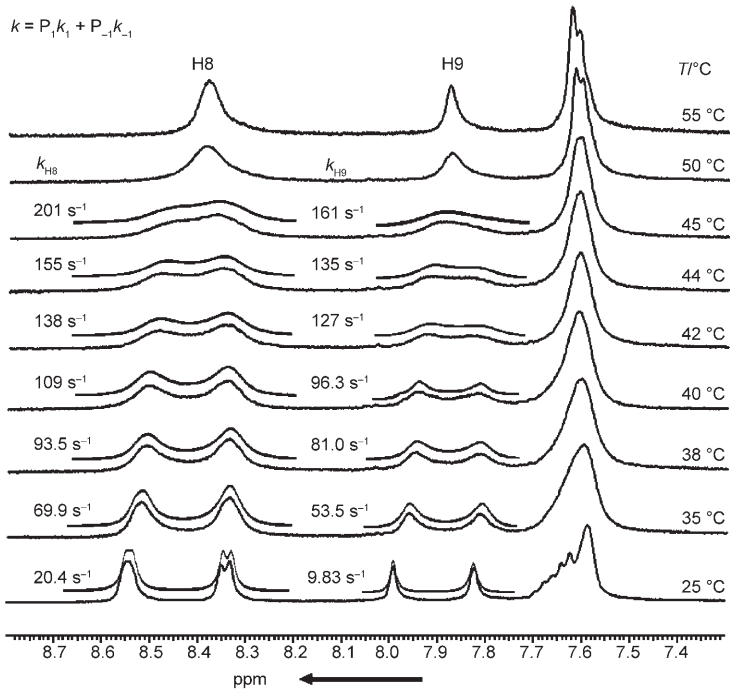

Figure 5. ^{1}H NMR temperature dependence of the H_8 and H_9 signals of **10** (9 mM) in D_2O.

On the other hand, when adamantan-1-ol was added as a competitor, the spectrum changed strikingly (Figure 3e). The H_8 and H_9 peaks corresponding to the self-included species conformer (● in Figure 3b) disappeared and new peaks appeared (that is, $\delta = 8.45$ ppm for H_8 and $\delta = 7.90$ ppm for H_9). Integration of H_9 for the non-included (or weakly associated; see below) species increased from 0.50 H to 0.79 H, while the new conformer accounted for only 0.21 H. One might expect that inclusion of adamantan-1-ol in the empty CD cavity should not modify the chemical shift of PBN, so the increase in intensity for H_9 can be attributed to competition between adamantan-1-ol and the self-included nitrone fragment, the latter being expelled out of the cavity. The presence of additional peaks can be ascribed to a species accommodating both the nitrone fragment and the adamantan-1-ol in the cavity. Unlike in the case of **7**, however, this species is minor, probably because the Me3CD cavity is less suited than the Me2CD cavity to accommodate both the nitrone and the adamantan-1-ol. The temperature dependence of H_8 and H_9 showed dramatic changes when the temperature was increased from 25 °C to 45 °C, at which the signals for non-included (or weakly associated; see below) and self-included species coalesce ($T_C \approx 45$ °C; Figure 5).

Fast versus slow exchange processes: As mentioned above, in the case of Me2CD-PBN (**7**) there was no temperature dependence of the H_8 and H_9 lines, which in general represents a fast exchange process on the NMR timescale. Such a fast exchange is the general case for host–guest interactions involving cyclodextrins as hosts.[25] On the other hand, the temperature dependencies of H_8 and H_9 observed for **10** are characteristic of slow exchange processes, which are less common for host–guest interactions involving cyclodextrins as hosts. Simulations of the NMR line-shapes of the signals (superimposed lines, Figure 5) were carried out with a 2D simulation program,[26] affording the rate constants k_1 for the self-inclusion (forward reaction) of the nitrone moiety inside the Me3CD cavity and k_{-1} for the exclusion (backward reaction), together with the corresponding populations (P_1, P_{-1}; see Supporting Information). The averaged values of k_1 and k_{-1} obtained for H_8 and H_9 were used to determine the Arrhenius (kinetic, frequency factors A and activation energies E_a, Figure 6 and Table 1) and Van't Hoff (thermodynamic, Gibbs energy ΔG_r, reaction enthalpy ΔH_r, and reaction entropy ΔS_r, Figure 6 and Table 1) reaction parameters. It is worth mentioning the enrichment of the non-associated species with increasing temperature (decrease in K). The thermodynamic parameters show that the self-inclusion reaction is enthalpically favoured ($\Delta H_r \approx -11\,\text{kJ mol}^{-1}$) but entropically ($\Delta S_r = -35.0\,\text{J K}^{-1}\text{mol}^{-1}$) compensated ($\Delta G_r \approx 0\,\text{kJ mol}^{-1}$).

This is typical of nonclassical hydrophobic interactions ($\Delta H_r \ll 0$, $T\Delta S_r \ll 0$).[27] The entropic cost can be ascribed

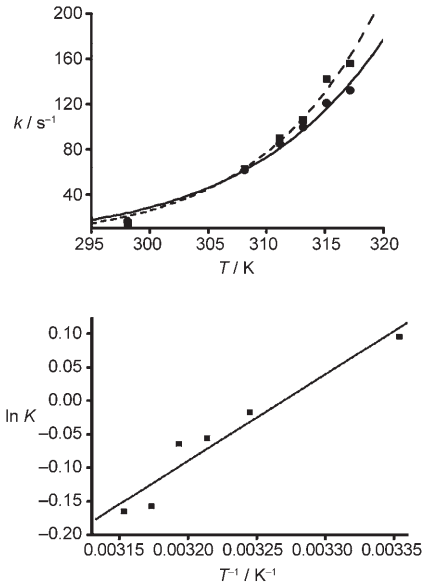

Figure 6. Arrhenius (top; ●: k_1, ■: k_{-1}) and Van't Hoff (bottom) plots for the out⇄in equilibrium of **10** in D_2O.

attributed to the energetic cost for the desolvation of the polar nitrone function for the forward reaction and to the loss of stabilizing van der Waals host–guest interactions for the backward reaction. In the latter case, the large positive value of $\Delta S^{\neq}_{-1}$ highlights a transition state less sterically hindered (loose TS) than the self-included species. Notably, an unexpected positive $\Delta S^{\neq}_{1}$ value for the forward reaction is observed, whereas one would expect a sterically hindered approach of the nitrone fragment ($\Delta S^{\neq}_{1} < 0$) due to shielding of the cavity entrance because of the methylation of the hydroxy groups. Indeed, the spacer holds the PBN fragment close to the entrance of the cavity (spacer effect), forcing inclusion of the PBN fragment deeper in the cavity, giving rise to a positive $\Delta S^{\neq}_{1}$ value.[29,30] Consequently, the expected entropic cost ($\Delta S^{\neq} < 0$) for the host–guest adaptation is overbalanced by the spacer effect. All these energetic observations are accounted for well by an out–in complex equilibrium: that is, an equilibrium between a deeply included nitrone fragment and a nitrone fragment close to the entrance of the cavity as displayed in Figure 7.

Table 1. Kinetic and thermodynamic parameters for the exchange process between the free and self-included conformers of Me3CDPBN (**10**) and Me3CDTIPNO (**11**) in water.

	ΔG_r[a,b]	ΔH_r[a]	ΔS_r[c]	E_a[d]	A[e]	$\Delta G^{\#}$[f,b]	$\Delta H^{\#}$[f]	$\Delta S^{\#}$[g]
10	−0.26	−10.7	−35.0	73.2[h]	1.6×10^{14}[h]	65.9[h]	84.4[h]	62.1[h]
				85.4[i]	1.9×10^{16}[i]	66.3[i]	96.5[i]	101.4[i]
11[j]	1.2	2.5	4.5	7.9[h]	12.6×10^{7}[h]	34.5[h]	4.8[h]	−104.5[h]
				5.4[i]	7.3×10^{7}[i]	33.3[i]	2.3[i]	−100.0[i]

[a] kJ mol^{-1}, error ca. 2 kJ mol^{-1}. [b] At 298 K. [c] J K^{-1} mol^{-1}, error ca. 5 J K^{-1} mol^{-1}. [d] kJ mol^{-1}, error ca. 8 kJ mol^{-1}. [e] In s^{-1}, error of a factor of 3. [f] kJ mol^{-1}, error ca. 7 kJ mol^{-1}. [g] J K^{-1} mol^{-1}, error ca. 20 J K^{-1} mol^{-1}. [h] Association process. [i] Dissociation process. [j] For molecule **11**, see ref. [16] and Figure 8.

Nitrone versus nitroxide inclusion-exclusion processes: In previous attempts to model the formyl ($CO_2^{\bullet-}$) and superoxide ($O_2^{\bullet-}$) spin-adducts, nitroxide **11**, Me3CD-TIPNO (Figure 8), was prepared and its inclusion-exclusion processes were studied by EPR.[16] Those data are now discussed both to the amide-type spacer and to the rigidity of the planar aromatic nitrone moiety, which reduces the mobility of the guest included in the cavity. Thus, the enthalpic gain due to the van der Waals interactions inside the cavity is merely sufficient to compensate the entropic cost due to the adoption of a strained supramolecular conformation. The Arrhenius parameters show large activation energies $E_{a,1}$ and $E_{a,-1}$ and unexpectedly high frequency factors A_1 and A_{-1} that are typical of a loose transition state. These high values might be partly due to the E_a–A compensation error effect,[28] and allowed only a qualitative discussion of the Eyring parameters $\Delta H^{\neq}$ and $\Delta S^{\neq}$. The large $\Delta H^{\neq}$ values are

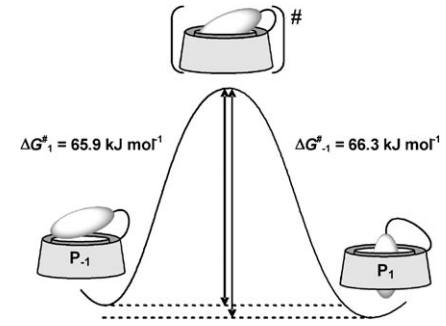

Figure 7. Reversible pathway from weakly to strongly associated PBN part for **10** in D_2O.

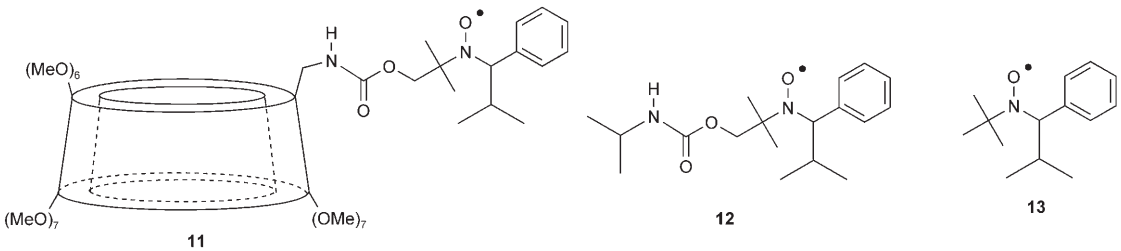

Figure 8. Nitroxide models **11**–**13** used for EPR study of the spin-adducts.

in comparison with those of **10**.

Dramatically different Arrhenius and Van't Hoff parameters were observed. In contrast to Me3CD-PBN (**10**), the non-included nitroxide fragment species is preferred over the self-included species ($\Delta G_r > 0$), and the ΔH_r and ΔS_r parameters exhibit positive values. However, the magnitudes for the parameters reported for **11** are clearly smaller than those observed for **10**, meaning small differences between the species involved in the exchange processes for **11**. In this case, the exchange process involves two conformers in equilibrium with the nitroxide fragment in non-included and in partly included (mainly lying in the middle of the methoxy crown of the Me3CD cavity) positions, in contrast with the equilibrium observed in the case of nitrone Me3CD-PBN (**10**). The negative $\Delta S_1^{\neq}$ observed for the exchange in **11** in contrast to **10** denotes a highly hindered TS, probably due both to the change in hybridization on the Cα carbon, from sp^2 in the nitrone moiety to sp^3 in the nitroxide moiety, and to the presence of the bulky isopropyl group in the β position. These two modifications make the forward reaction (inclusion process) for **11** more sensitive to steric hindrance, due to the methoxy crown shielding the entrance of the cavity. Furthermore, $\Delta H_1^{\neq}$ is clearly smaller for **11** than for **10**, as would be expected for an easier desolvation of the less polar nitroxide function. However, for the included nitroxide fragment of **11**, one would expect a larger $\Delta H_{-1}^{\neq}$ value than for **10**, because of stronger stabilizing van der Waals interactions between the apolar cavity and the nitroxide fragment, which is less polar than the nitrone moiety. Hence, the smaller $\Delta H_{-1}^{\neq}$ for the exclusion of nitroxide than for the nitrone fragment is consistent with weak van der Waals interactions, as would be expected for the nitroxide part lying in the methoxy crown.

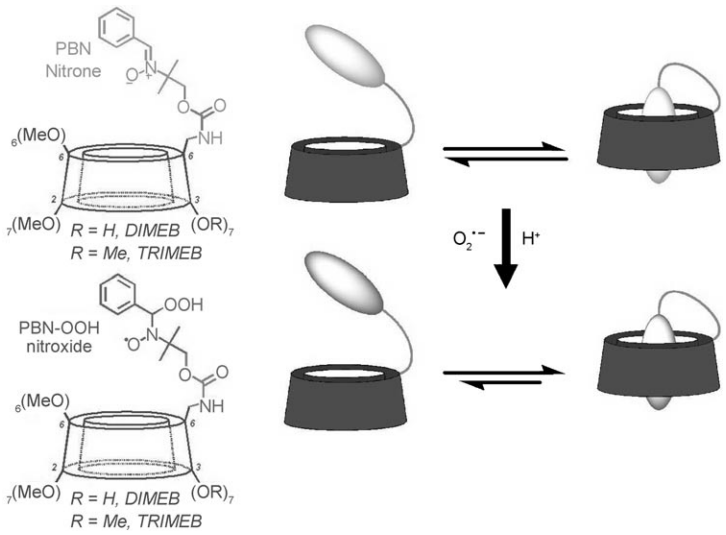

Scheme 2. Proposed general situation for nitrone and nitroxide self-inclusion equilibria prior to (top) and after (bottom) superoxide spin-trapping by CD-functionalized spin-traps **7** and **10**.

Spin-trapping experiments with Me2CD-PBN (7) and Me3CD-PBN (10): In previous studies involving bimolecular complexes, we have shown that the PBN–superoxide nitroxide spin-adducts associate more strongly than the parent PBN nitrones with methylated β-cyclodextrins.[11] Hence, one might expect the spin-adducts obtained by spin-trapping with covalent nitrones **7** and **10** to exhibit greater persistence, due both to conformational changes decreasing fragmentation reactions[31] and to the self-inclusion of the nitroxide fragment, making the bioreduction less efficient (Scheme 2).

$CO_2^{\bullet-}$ spin-trapping EPR experiments: Spin-trapping of a carbon-centred radical such as $CO_2^{\bullet-}$, which commonly gives persistent spin-adducts with intense EPR signals, was first investigated with both the bimolecular PBN/TRIMEB and the unimolecular Me3CD-PBN (**10**) systems to check the spin-trapping efficiency of molecule **10**. The bimolecular PBN/TRIMEB was studied first (entries 1 and 2, Table 2) with equimolar amounts of spin-trap and host. The EPR parameters were obtained with the assumption of an exchange between a non-included (entry 1, Table 2) and an included (entry 2, Table 2) species. In contrast with the EPR model experiments performed with nitroxides **12** and **13** (Figure 8, $\Delta a_N = 0.04$ mT)[16] in the presence of TRIMEB, the observed $\Delta a_N = 0.015$ mT is rather small, probably denoting a partly included nitroxide fragment. Surprisingly, the relaxation parameters α, β and γ are larger for the free spin-adduct PBN-$CO_2^{\bullet-}$ than for the supramolecular spin-adduct PBN-$CO_2^{\bullet-}$/

Table 2. EPR parameters for the exchange between the free and the partly included forms of the $CO_2^{\bullet-}$ adducts of PBN/TRIMEB and **10** systems in phosphate buffer (pH 7.4).

Entry	Spin-adduct	a_N[a] [mT]	$a_{\beta,H}$[a] [mT]	α[a] [mT]	β[a] [mT]	γ[a] [mT]
1	TRIMEB/PBN-$CO_2^{\bullet-}$[b]	1.581	0.322	0.137	0.040	0.047
2	TRIMEB/PBN-$CO_2^{\bullet-}$[c]	1.566	0.338	0.048	0.006	0.005
3	**10**-$CO_2^{\bullet-}$[d,e]	1.512	0.300	0.217	0.062	0.077
4	**10**-$CO_2^{\bullet-}$[d,f]	1.494	0.310	0.092	0.036	0.035

[a] Nitrogen a_N and β-hydrogen $a_{\beta,H}$ hyperfine coupling constants, and relaxation parameters α, β, and γ are determined as in ref. [16]. [b] Free spin-adduct. [c] Included spin-adduct. [d] Concentration of **10** in the 3.5 to 25 mM range. [e] Non-included spin-adduct fragment. [f] Partly self-included spin-adduct fragment.

TRIMEB, whereas one would expect a slower rotational motion for the supramolecular system than for the free spin-adduct. This might be explained by the strong solvation of the carboxylate group making small molecules resemble large ones, whereas inclusion into the cavity of TRIMEB involves a partial desolvation of the spin-adduct. Hence, the solvation being smaller for the supramolecular system, the rotation motion is easier and the relaxation parameters are smaller (entry 2, Table 2).

With concentrations of **10** in the 3.5 to 25 mM range, intense EPR signals exhibiting strong distortion were recorded. The absence of changes in the EPR features with dilution was consistent with an intramolecular association process. The strongly distorted signals are due to species experiencing strongly impeded rotational motion, specific of large molecules (Figure 9).

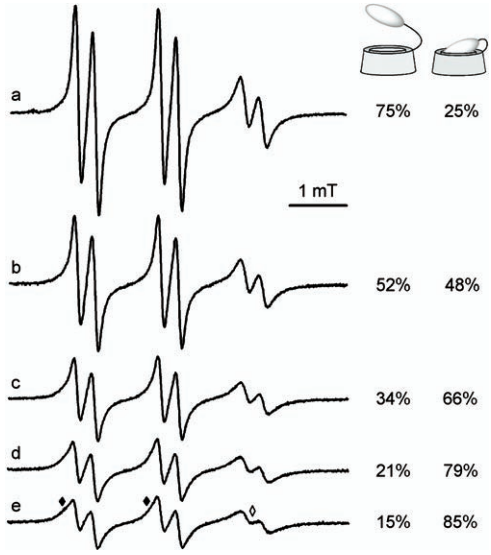

Figure 9. Evolution of the Me3CD-PBN-$CO_2^{\bullet-}$ spin-adduct EPR spectrum and calculated proportions between included and non-included nitroxides within the timescales: a) 90 s, b) 180 s, c) 300 s, d) 420 s, and e) 540 s.

EPR data were therefore obtained by spectrum simulations with the assumption of the existence of two species, one with non-included and one with (partly) partly self-included spin-adduct fragments. As in the cases of the bimolecular system and the nitroxide model **11** ($\Delta a_N = 0.03$ mT), the small $\Delta a_N = 0.018$ mT between these two species (entries 3 and 4, Table 2) led us to assume an equilibrium between a non-included and a partly self-included species. The spin-adduct fragment is probably lying in the methoxy crown of the narrow ring. Such a form of partial inclusion is due both to the bulkiness of the solvated COO^- group and to the disfavoured desolvation of the polar COO^- moiety impeding the inclusion of the spin-adduct fragment. An increase in the polarity of the spin-adduct fragment is also likely to weaken the stabilizing van der Waals interactions. The relaxation parameters for the non-included and self-included species exhibit the same trends as already observed for the nitroxide model **11** and so need no further comments. On the other hand, after 450 s, the global intensities of the signals had decreased by ca. 40% in the case of the spin-adduct **10**-$CO_2^{\bullet-}$ and by ca. 60% in that of the bimolecular spin-adduct system PBN-$CO_2^{\bullet-}$/TRIMEB, but were almost unchanged in that of the free PBN-$CO_2^{\bullet-}$ spin-adduct. It is noteworthy that the separate evolution of the two spin-adducts of **10** shows a faster decay for the non-included species than for the partly included one, leading to an artificial enrichment in the partly self-included species. In this case, the presence of cyclodextrin—attached or not attached—to the nitrone is detrimental to the persistence of the formate spin-adduct. As the occurrence of fast side-reactions between the nitroxide moiety and the CD moiety are unlikely at room temperature, the faster decay may thus be due to conformational changes facilitating, for example, a CD-catalysed β-fragmentation (i.e., back reaction) of the formyl group.[31] In the case of a bimolecular system, the slight increase in $a_{H,\beta}$ (although a decrease would be expected, due to the decrease in spin density on the nitrogen atom: $\Delta a_N > 0$), denotes conformational changes around the nitroxide moiety. That is, the increase in $a_{H,\beta}$ may involve a decrease in the $<H_\beta$-C-N-2p$>$ dihedral angle and consequently a decrease in the $<$2p-N-C-$CO_2^{\bullet}>$ dihedral angle, which may favour overlapping between σ*C–CO_2^- and the 2p orbital containing the odd spin density, hence accelerating the β-fragmentation reaction. On the other hand, the presence of the bulky CD and the positioning of the nitrone fragment close to the cavity probably induced diastereoselective scavenging. Thus, because of the steric hindrance of the CD, the nitroxide moiety probably adopted different conformations for partly included and non-included forms—as highlighted by the small changes in $a_{H,\beta}$—leading to less stable non-included species for the same reasons as described for the bimolecular system. Nevertheless, Me3CD-PBN (**10**) appears to be an efficient trap for the formyl radical, in spite of the significant nitrone self-association.

$O_2^{\bullet-}$ spin-trapping EPR experiments: In absence of CD, the intensity of the EPR signal of the PBN superoxide (PBN-OOH) spin-adduct is very weak and disappears in less than one minute (Figure 10a).

On the other hand, a longer persistence and a higher EPR signal intensity of the PBN-OOH spin-adduct in the presence of a cyclodextrin derivative—TRIMEB (Figure 10b) or DIMEB (Figure 10d)—were observed for the bimolecular PBN/CD systems, with DIMEB affording the more intense signal and the more persistent supramolecular spin-adduct. The same trends are observed for the superoxide spin-adducts with the covalent molecules **10** (Figure 10c) and **7** (Figure 10e). Moreover, the signals are more intense for the monomolecular systems than for the bimolecular ones, owing to the forced host–guest proximity, which favours the self-inclusion processes. However, whatever the system—bimolecular or monomolecular-–and the type of CD derivative—DIMEB or TRIMEB—the decay of the

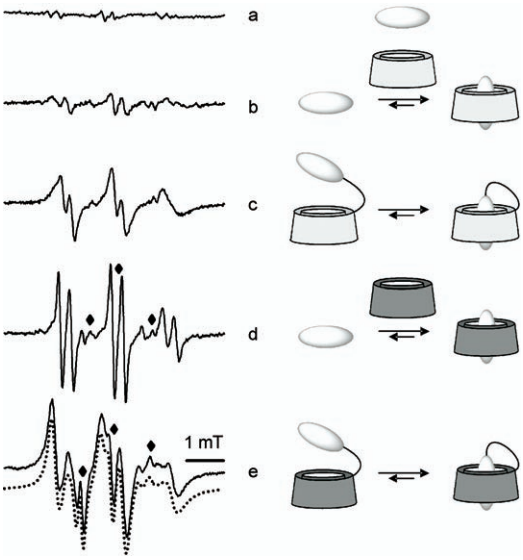

Figure 10. Differences in EPR signal shapes and intensities of $O_2^{\bullet-}$ spin-adducts as a function of the spin-trap system: a) PBN alone (25 mM), b) PBN/TRIMEB (25/25 mM), c) **10** (25 mM), d) PBN/DIMEB (25/25 mM), and e) **7** (25 mM). (◆) = three-lines EPR signal attributed to the acyl-type decomposition product,[11] —— = experimentally measured spectra, ••••• = simulated spectrum. Truncated cones are used to symbolize CD derivatives, and egg shapes for PBN or spin-adduct.

spin-adduct generated a three-line signal ascribed to an acyl-type nitroxide.[11] Such signals arose from the sequential H_β abstraction and β-fragmentation of the hydroperoxide group. Determination of reliable and accurate EPR parameters by simulation of **10**-OOH spin-adduct EPR spectra was not possible because of the broad linewidths ($\Delta H_{pp} \approx 0.14$–0.18 mT). However, the large anisotropy of the signal at high field underlines the presence of the self-included spin-adduct fragment as already observed in the case of the nitroxide model **11**. On the other hand, in the case of the spin-adduct **7**-OOH, simulations afforded clear evidence for an exchange between two species. Furthermore, the value of $\Delta a_N = 0.075$ mT is unambiguously larger than the value $\Delta a_N = 0.054$ mT for the PBN-OOH ($a_N = 1.480$ mT) and the 1:2 complex DIMEB/PBN-OOH/DIMEB ($a_N = 1.426$ mT), and also strikingly larger than the $\Delta a_N = 0.018$ mT for the **10**-CO_2H spin-adduct species. Consequently, such a large Δa_N value suggests an equilibrium between non-included (entry 1, Table 3) and deeply self-included (entry 2, Table 3)

Table 3. EPR parameters for the exchange between the non-included and the self-included conformers of the superoxide spin-adduct of **7** in phosphate buffer (pH 7.4).

Entry	Species	a_N[a] [mT]	$a_{H,\beta}$[a] [mT]	ν[a] [mT]	%
1	**7**-OOH[b,c]	1.415	0.32	0.20	73
2	**7**-OOH[b,d]	1.340	0.55	0.13	20
3	acyl nitroxide[e]	0.815	–[f]	0.10	7

[a] Nitrogen a_N and β-hydrogen $a_{H,\beta}$ hyperfine coupling constants, and relaxation parameter ν given by the simulation program as in ref. [16]. [b] [**7**] = 25 mM. [c] Non-included spin-adduct fragment. [d] Self-included spin-adduct fragment. [e] Degradation product. [f] No hydrogen in position β; see text.

species. This sharp contrast between the two spin-adducts **7**-OOH and **10**-$CO_2^{\bullet-}$ is probably due both to the better complexing properties of the Me2CD over Me3CD and to the trapped radical. However, the self-included/non-included spin-adduct fragment ratio is in favour of the non-included species (75%), probably because of the disfavoured desolvation of the polar and protic OOH group. Nonetheless, superoxide spin-adducts of **7** and **10** led to more persistent species that were detectable up to 10 minutes after their generation

Spin-adduct reduction by sodium L-ascorbate: The persistence of the superoxide spin-adducts obtained with **7** and **10** was measured in the presence of L-ascorbate (0.1 mM) to mimic the physiological reductive conditions that destroy the nitroxide. Despite the observed higher signal intensities and longer persistence of the superoxide spin-adducts, no significant lifetime enhancements were observed, meaning that the resistance to L-ascorbate reductive conditions was not higher for monomolecular systems than it was for bimolecular systems. Improvements were attempted by the addition of extra DIMEB (50 mM) to the superoxide spin-adducts of **7** and **10** (see Supporting Information), leading to an increase in the EPR spectrum intensity for the **7**-OOH spin-adduct and also to a slight one for the **10**-OOH spin-adduct. However, the half-life times of these species were not longer than one minute, as observed without addition of DIMEB.

As stated above, the non-included species was favoured over the self-included species, indicating that the complexation rate was low and could probably not compete with the high reduction rate. Consequently, the spin-adduct was strongly exposed to fast reductants such as sodium L-ascorbate and no effect due to the inclusion process was observed.

Conclusion

The first grafting of a nitrone onto β-cyclodextrins has been achieved under mild conditions that preserved the nitrone functionality, affording the PBN-derived DIMEB and TRIMEB derivatives as spin-traps for superoxide and formyl radical spin-trapping. NMR studies of the CD-PBN derivatives **7** and **10** showed that the nitrone moiety is in each case strongly self-included in the corresponding cavity. However, this inclusion process does not preclude efficient spin-trapping of the superoxide and formyl radicals whatever the spin-trap considered (**7** or **10**), as demonstrated by EPR spectroscopy. The resulting spin-adducts even exhibited enhanced EPR signals in relation to the noncovalent CD–nitrone systems or the nitrone alone used as spin-traps. Moreover, the half-life times for both supramolecular superoxide spin-adducts were significantly increased, but no effect on their bioreduction in the presence of L-ascorbate was detected. These results demonstrate that cyclodextrin grafting does not affect the spin-trapping properties of well known spin-traps and can afford additional benefits due to

the proximal positions of the cyclodextrin hosts as supramolecular protectors.

Acknowledgement

The financial support provided by the Conseil Régional Provence Alpes Côte d'Azur, the CNRS, the Université de Provence and TROPHOS Company (Marseille) is gratefully acknowledged.

[1] a) W. Dröge, *Physiol. Rev.* **2002**, *82*, 47–95; b) J. Foreman, V. Demidchik, J. H. F. Bothwell, P. Mylona, H. Miedema, M. A. Torres, P. Linstead, S. Costa, C. Brownlee, J. D. G. Jones, J. M. Davies, L. Dolan, *Nature* **2003**, *422*, 442–446; c) Y. Shibata, R. Branicky, I. O. Landaverde, S. Hekimi, *Science* **2003**, *302*, 1779–1782.

[2] a) M. P. Mattson, *Nature* **2004**, *430*, 631–639; b) E. Gaggelli, H. Kozlowski, D. Valensin, G. Valensin, *Chem. Rev.* **2006**, *106*, 1995–2044; c) M. T. Lin, M. F. Beal, *Nature* **2006**, *443*, 787–795.

[3] S. Cuzzocrea, E. Mazzon, L. Dugo, R. Di Paola, A. P. Caputi, D. Salvemini, *FASEB J.* **2004**, *18*, 94–101.

[4] J. H. J. Hoeijmakers, *Nature* **2001**, *411*, 366–374.

[5] a) M. Brownlee, *Diabetes* **2005**, *54*, 1615–1625; b) N. Houstis, E. D. Rosen, E. S. Lander, *Nature* **2006**, *440*, 944–948.

[6] a) H. Sies, *Angew. Chem.* **1986**, *98*, 1061–1076; *Angew. Chem. Int. Ed. Engl.* **1986**, *25*, 1058–1071; b) D. L. Korthuis, D. L. Carden, D. N. Granger, *Biological consequences of oxidative stress*, Oxford University Press, London **1992**, p. 50; c) H. Wiseman, B. Halliwell, *Biochem. J.* **1996**, *313*, 17–29; d) B. Kalyanaraman, *Oxygen Radicals, Disease and Disease Process* (Ed.: C. E. Thomas), Harwood, Amsterdam, **1997**.

[7] a) D. Salvemini, Z.-Q. Wang, J. L. Zweier, A. Samouilov, H. Macarthur, T. P. Misko, M. G. Currie, S. Cuzzocrea, J. A. Sikorski, D. P. Riley, *Science* **1999**, *286*, 304–306; b) M. J. Davies, G. S. Timmins, *Electron Paramagn. Reson.* **2000**, *17*, 1–42.

[8] a) J.-M. Lehn, *Supramolecular Chemistry*, VCH, Weinheim, **1995**; b) J. W. Steed, J. L. Atwood, *Supramolecular Chemistry*, Wiley-VCH, London, **2000**.

[9] H. Karoui, A. Rockenbauer, S. Pietri, P. Tordo, *Chem. Commun.* **2002**, 3030–3031.

[10] H. Karoui, P. Tordo, *Tetrahedron Lett.* **2004**, *45*, 1043–1045.

[11] D. Bardelang, A. Rockenbauer, J.-P. Finet, H. Karoui, P. Tordo, *J. Phys. Chem. B* **2005**, *109*, 10521–10530.

[12] D. Bardelang, A. Rockenbauer, H. Karoui, J.-P. Finet, I. Biskupska, K. Banaszak, P. Tordo, *Org. Biomol. Chem.* **2006**, *4*, 2874–2882.

[13] DIMEB is an acronym used to describe 2,6-di-*O*-Me-β-cyclodextrin and TRIMEB for the analogous 2,3,6-permethylated β-cyclodextrin. In this paper we use Me2CD and Me3CD to describe DIMEB or TRIMEB derivatives in which one 6-MeO has been replaced by a PBN-derived moiety.

[14] D. Bardelang, J.-L. Clement, J.-P. Finet, H. Karoui, P. Tordo, *J. Phys. Chem. B* **2004**, *108*, 8054–8061.

[15] H. G. Aurich, *Nitrones, Nitronates and Nitroxides*, Wiley, New York, **1989**.

[16] The resulting grafted nitroxide was demonstrated to self-associate in the TRIMEB cavity as a model of a trapped isopropyl radical by Me3CD-PBN (**10**): see D. Bardelang, A. Rockenbauer, L. Jicsinszky, J.-P. Finet, H. Karoui, S. Lambert, S. R. A. Marque, P. Tordo, *J. Org. Chem.* **2006**, *71*, 7657–7667. For other work on nitroxide spin-labelled cyclodextrins see a) R. M. Paton, E. T. Kaiser, *J. Am. Chem. Soc.* **1970**, *92*, 4723–4725; b) G. Ionita, V. Chechik, *Org. Biomol. Chem.* **2005**, *3*, 3096–3098; c) V. Chechik, G. Ionita, *Org. Biomol. Chem.* **2006**, *4*, 3505–3510.

[17] H. Parrot-Lopez, H. Galons, S. Dupas, M. Miocque, G. Tsoucaris, *Bull. Soc. Chim. Fr.* **1990**, *127*, 568–571.

[18] L. Jicsinszky, R. Iványi, *Carbohydr. Polym.* **2001**, *45*, 139–145.

[19] R. S. Macomber, *J. Chem. Educ.* **1992**, *69*, 375–378.

[20] K. A. Connors, *Binding Constants: the measurement of molecular complex stability*, Wiley, New York, **1987**.

[21] K. A. Connors, *Chem. Rev.* **1997**, *97*, 1325–1357.

[22] The H_9 chemical shift was determined unambiguously at 7.50 ppm by a HMQC sequence and by comparing the observed cross correlations with those of the PBN in water. However a satisfactory ^{13}C NMR spectrum of **7** could not be obtained in spite of a 50 mM concentration and 3072 scans.

[23] M. V. Rekharsky, Y. Inoue, *Chem. Rev.* **1998**, *98*, 1875–1917.

[24] a) T. Haino, D. M. Rudkevich, J. Rebek, Jr., *J. Am. Chem. Soc.* **1999**, *121*, 11253–11254; b) S. M. Biros, J. Rebek, Jr., *Chem. Soc. Rev.* **2007**, *36*, 93–104.

[25] H. J. Schneider, F. Hacket, V. Rüdiger, H. Ikeda, *Chem. Rev.* **1998**, *98*, 1755–1785.

[26] A. Rockenbauer, L. Korecz, *Appl. Magn. Reson.* **1996**, *10*, 29–43.

[27] E. A. Meyer, R. K. Castellano, F. Diederich, *Angew. Chem.* **2003**, *115*, 1244–1287; *Angew. Chem. Int. Ed.* **2003**, *42*, 1210–1250.

[28] K. Héberger, S. Kemény, T. Vidoczy, *Int. J. Chem. Kinet.* **1987**, *19*, 171–181.

[29] P. Franchi, M. Lucarini, G. F. Pedulli, D. Sciotto, *Angew. Chem.* **2000**, *112*, 269–272; *Angew. Chem. Int. Ed.* **2000**, *39*, 263–266.

[30] S. Saudan, F. A. Dunand, A. Abou-Hamdan, P. Bugnon, P. G. Lye, S. F. Lincoln, A. E. Merbach, *J. Am. Chem. Soc.* **2001**, *123*, 10290–10298.

[31] The main decay process of the glutathiyl spin-adduct of PBN is the fragmentation reaction regenerating the thiyl radical and the PBN. This reaction is slowed down several times for the corresponding spin-adduct of **7**. Personal communication from Prof. E. G. Bagryanskaya (Novosibirsk).

Received: March 5, 2007
Published online: August 29, 2007

